Immunity, Volume *50*

Supplemental Information

Microbiota Sensing by Mincle-Syk Axis in Dendritic Cells Regulates Interleukin-17 and -22 Production and Promotes Intestinal Barrier Integrity

María Martínez-López, Salvador Iborra, Ruth Conde-Garrosa, Annalaura Mastrangelo, Camille Danne, Elizabeth R. Mann, Delyth M. Reid, Valérie Gaboriau-Routhiau, Maria Chaparro, María P. Lorenzo, Lara Minnerup, Paula Saz-Leal, Emma Slack, Benjamin Kemp, Javier P. Gisbert, Andrzej Dzionek, Matthew J. Robinson, Francisco J. Rupérez, Nadine Cerf-Bensussan, Gordon D. Brown, David Bernardo, Salomé LeibundGut-Landmann, and David Sancho

SUPPLEMENTAL INFORMATION

Table S1: Primer sequences for quantitative PCR. Related to STAR Methods.

Gene	Forward (5´-3´)	Reverse (5´-3´)	Source
Gadph	TGAAGCAGGCATCTGAGGG	CAGGAAGTAGGTGAGGGCTTG	(Sancho et al., 2009)
Clec4e	AGTGCTCTCCTGGACGATAG	CCTGATGCCTCACTGTAGCAG	(Zhao et al., 2014)
Tgfb	GCATGGCTGAACCAAGGA	AAAGAGCAGTGAGCGCTGAATC	This paper
Il6	CCGTGTGGTTACATCTACCCT	CGTGGTTCTGTTGATGACAGT	(Conejero et al., 2017)
Il23a	TGCTGGATTGCAGAGCAGTAA	GCATGCAGAGATTCCGAGAGA	This paper
Il12b	GGAAGCACGGCAGCAGAATA	AACTTGAGGGAGAAGTAGGAATGG	(Martinez-Lopez et al., 2015)
Reg3g	TTCCTGTCCTCCATGATCAAA	CATCCACCTCTGTTGGGTTC	(Vaishnava et al., 2011)
Saa1	CATTTGTTCACGAGGCTTTCC	GTTTTTCCAGTTAGCTTCCTTCATGT	(Goto et al., 2014)
Bactin	GGCTGTATTCCCCTCCATCG	CCAGTTGGTAACAATGCCATGT	(Martinez-Lopez et al., 2015)
Acc	GATGAACCATCTCCGTTGGC	GACCCAATTATGAATCGTG	(Zhao et al., 2016)
Ppara	ACAAGGCCTCAGGGTACCA	GCCGAAAGAAGCCCTTACA	This paper
Fas	GCGGGTTCGTGAAACTGATAA	GCAAAATGGGCCTCCTTGATA	(Matesanz et al., 2018)
Scd1	TTCTTGCGATACACTCTGGTGC	CGGGATTGAATGTTCTTGTCGT	(Matesanz et al., 2018)
Srebpc	GGCACTGAAGCAAAGCTGAA	TCATGCCCTCCATAGACACA	This paper
Pepck	CCATCACCTCCTGGAAGAACA	ACCCTCAATGGGTACTCCTTCTG	(Matesanz et al., 2018)
Cpt1a	CTCCGCCTGAGCCATGAAG	CACCAGTGATGATGCCATTCT	(Matesanz et al., 2018)
G6pase	CGACTCGCTATCTCCAAGTGA	GTTGAACCAGTCTCCGACCA	(Matesanz et al., 2018)
SFB	TGTGGGTTGTGAATAACAAT	GCGAGCTTCCCTCATTACAAGG	(Snel et al., 1995)
16S Amplicon	TCGTCGGCAGCGTCAGATGTGTATA AGAGACAGCCTACGGGNGGCWGCAG	GTCTCGTGGGCTCGGAGATGTGTATAAGAGAC AGGACTACHVGGGTATCTAATCC	(Klindworth et al., 2013)

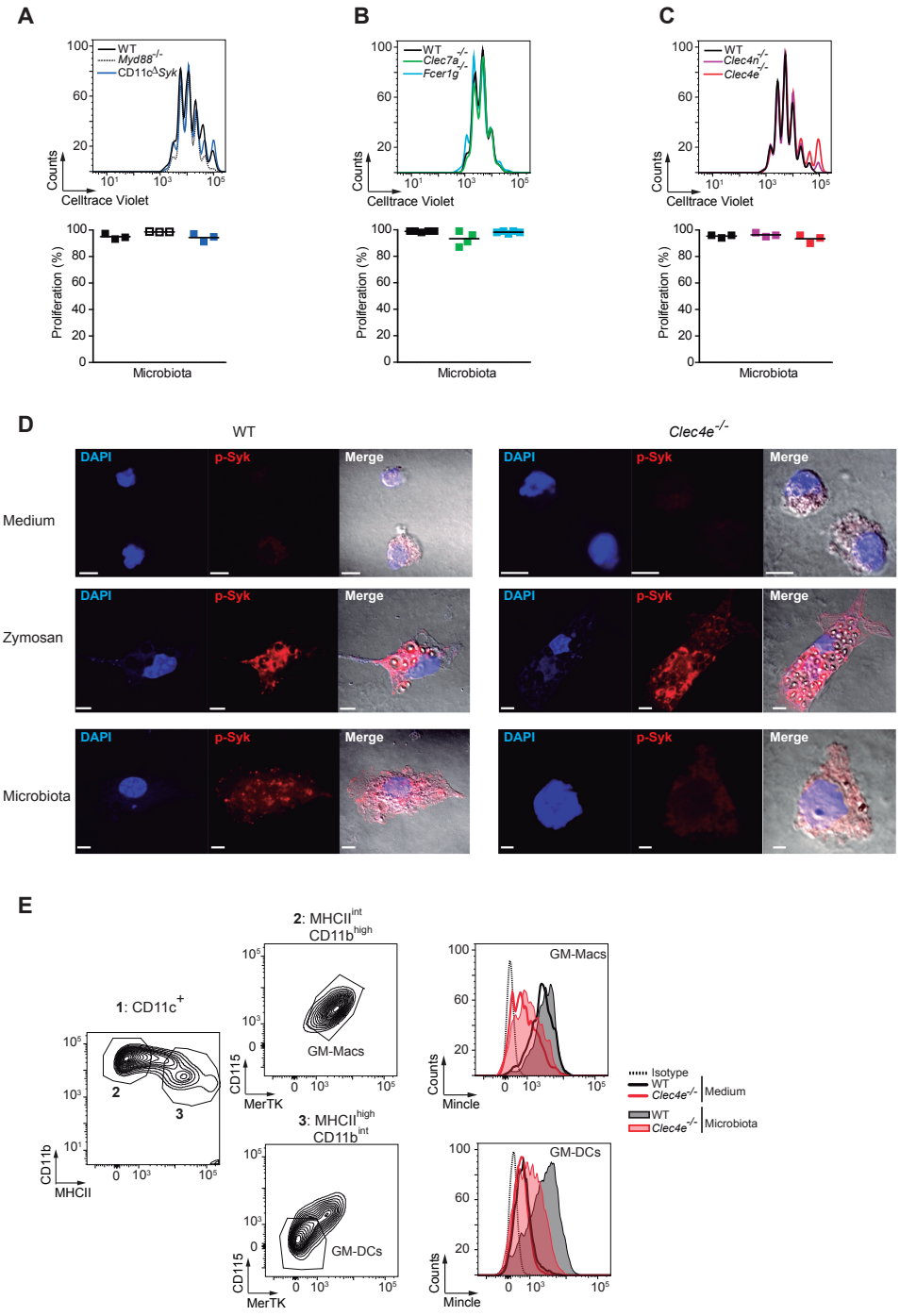

Figure S1. Mincle and Syk in DCs mediate microbiota-induced Th17 differentiation. Related to Figure 1. (A-C) Top: Representative FACS plots showing Celltrace Violet dilution in OT-II T cells co-cultured with GM-BMs from the indicated genotypes previously stimulated with gut microbiota (10:1 GM-BM ratio) and loaded with $OVA_{323-339}$ peptide. Bottom: Quantification of proliferation. (D) Representative confocal images of Syk phosphorylation (red) in GM-BMs from WT and Mincle-deficient (*Clec4e*$^{-/-}$) mice, 30 minutes after stimulation or not (medium) with zymosan (10 µg/mL) or gut microbiota (10:1 GM-BM ratio). DAPI was used for nuclear counterstaining. Merged image with DAPI, P-Syk and visible; (scale bar = 5 µm; *Clec4e*$^{-/-}$ plus microbiota : 2 µm) (E) Left: Gating strategy used to sort GM-macrophages (GM-Macs) and –DCs (GM-DCs) from GM-BMs. Right: Representative histograms showing Mincle or isotype staining for the indicated populations. (A-E) One representative experiment of at least three performed.

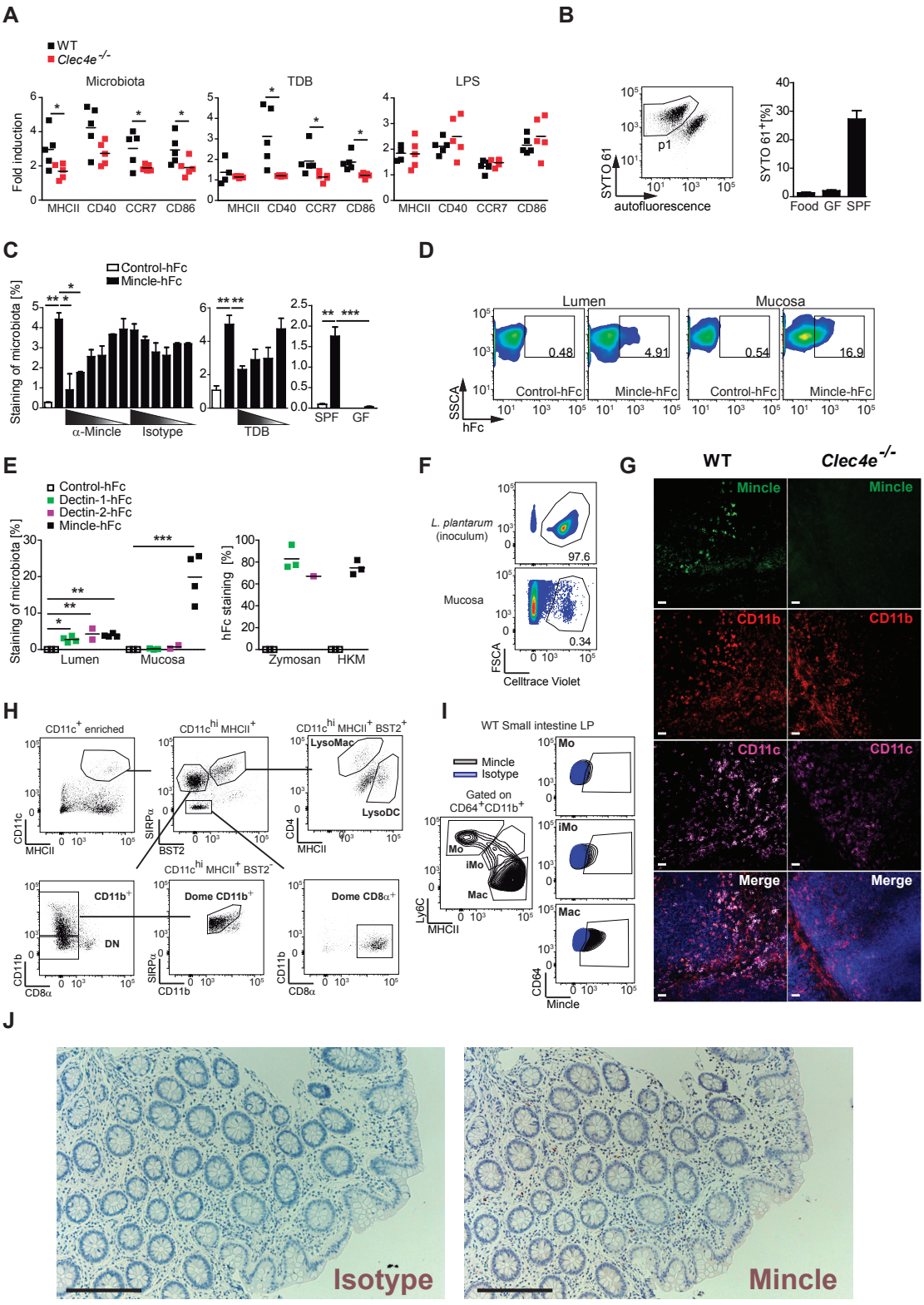

Figure S2. Mucosa-associated commensals are sensed by Peyer´s patches DCs expressing Mincle. Related to Figure 2. (A) MHCII, CD40, CCR7 and CD86 expression measured by flow cytometry in GM-BMs from WT and Mincle-deficient (*Clec4e*$^{-/-}$) mice exposed for 12 hours to gut microbiota (10:1 GM-BM ratio), plated TDB (1µg/well) or LPS (100 ng/ml). Graph shows fold induction of the indicated markers, calculated as the treated vs. untreated MFI (Mean Fluorescence Intensity) ratio. Each point represents an independent GM-BM culture from a different mouse (biological replicates). Individual data and arithmetic mean from one representative experiment of two independent experiments are shown (B) Gating strategy for the analysis of the intestinal microbiota by flow cytometry. Commensal microbes were labeled with cell

permeant SYTO 61 fluorescent nucleic acid stain. Left: representative FACS plots. Right: Summary graph showing percentages of SYTO 61-labelled microorganisms in the indicated samples. Each bar is the mean + SEM of 2 samples of food, or 8 Germ free (GF) or SPF (Specific pathogen free) mice. (C) Frequency of microbiota stained with Control-hFc or Mincle-hFc as indicated. Left: after pre-incubation with titrated dilutions of anti-human Mincle (clone 2F2) or an isotype control antibody; middle: after pre-incubation with decreasing doses of TDB (half dilution starting 1 mg/ml); right: in the intestinal content from SPF and GF mice. (D) Representative plots showing the luminal (left) or mucosal (right) microorganisms labelled with Control-hFc or Mincle-hFc. (E) Left: Frequency of luminal or mucosa-associated microbiota stained with the indicated Fc chimeras. Right: Frequency of zymosan or Heat-killed *Mycobacterium* (HKM) stained with the indicated hFc chimeras. (F) Representative plot of *Lactobacillus plantarum* (*L. plantarum*) labeled with Celltrace Violet prepared for oral gavage (left) or recovered from the mucosa 6 hours after oral inoculation (right). (G) Representative confocal images showing whole mount preparations of PPs from WT and Mincle-deficient (*Clec4e*$^{-/-}$) mice stained with anti-Mincle antibody (clone 1B6) (green), CD11b (red) and CD11c (pink) co-stained with DAPI (blue); (scale bar = 20 μm). (H) Gating strategy employed for myeloid cells analysis in mouse PPs. (I) Left: Gating strategy used to identify the small intestine mouse LP Monocytes (Mo), intermediates Mo (iMo) and Macrophages (Mac). Right: Representative dot plot showing Mincle expression (black) or its isotype control (blue) in the indicated populations. (J) Immunohistochemistry analysis of normal human ascending colon using anti-human Mincle antibody (clone 2A8) or its isotype. Upper part (scale bar = 100 μm) (A-D, F-J) One representative experiment of two performed. (E) Pool of two independent experiments. * $p < 0.05$; ** $p < 0.01$; *** $p < 0.001$ (A,C) Unpaired two-tailed Student´s t test; (E) One-way ANOVA and Bonferroni post-hoc test.

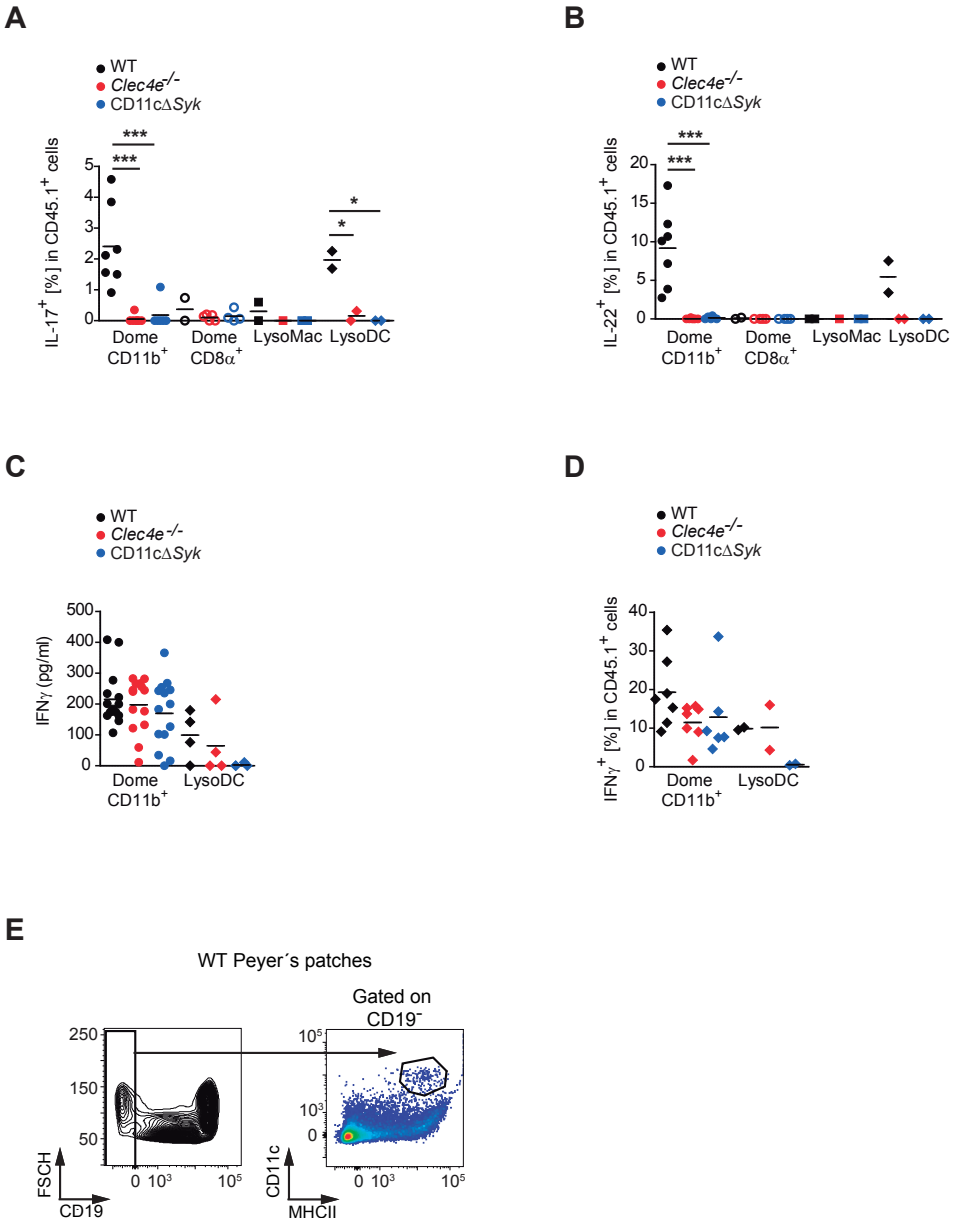

Figure S3. Peyer's patches DCs instruct Mincle and Syk-dependent Th17 without affecting Th1 differentiation. Related to Figure 3. (A-D) Naïve OT-II T cells co-culture with sorted dome CD11b$^+$ DCs, CD8α$^+$ DCs, LysoMacs or LysoDCs from PPs. Summary graph showing the percentage of IL-17$^+$ (A) or IL-22$^+$(B) after PMA and ionomycin stimulation measured by intracellular staining and flow cytometry. IFN-γ production by ELISA (C) or after PMA and ionomycin stimulation (D). (E) Gating strategy used to analyze cytokine production shown in Figure 3E and F. (C) Two independent pooled experiments. (A,B,D,E) One representative experiment of at least three performed. * $p < 0.05$; *** $p < 0.001$ (One-way ANOVA and Bonferroni post-hoc test)

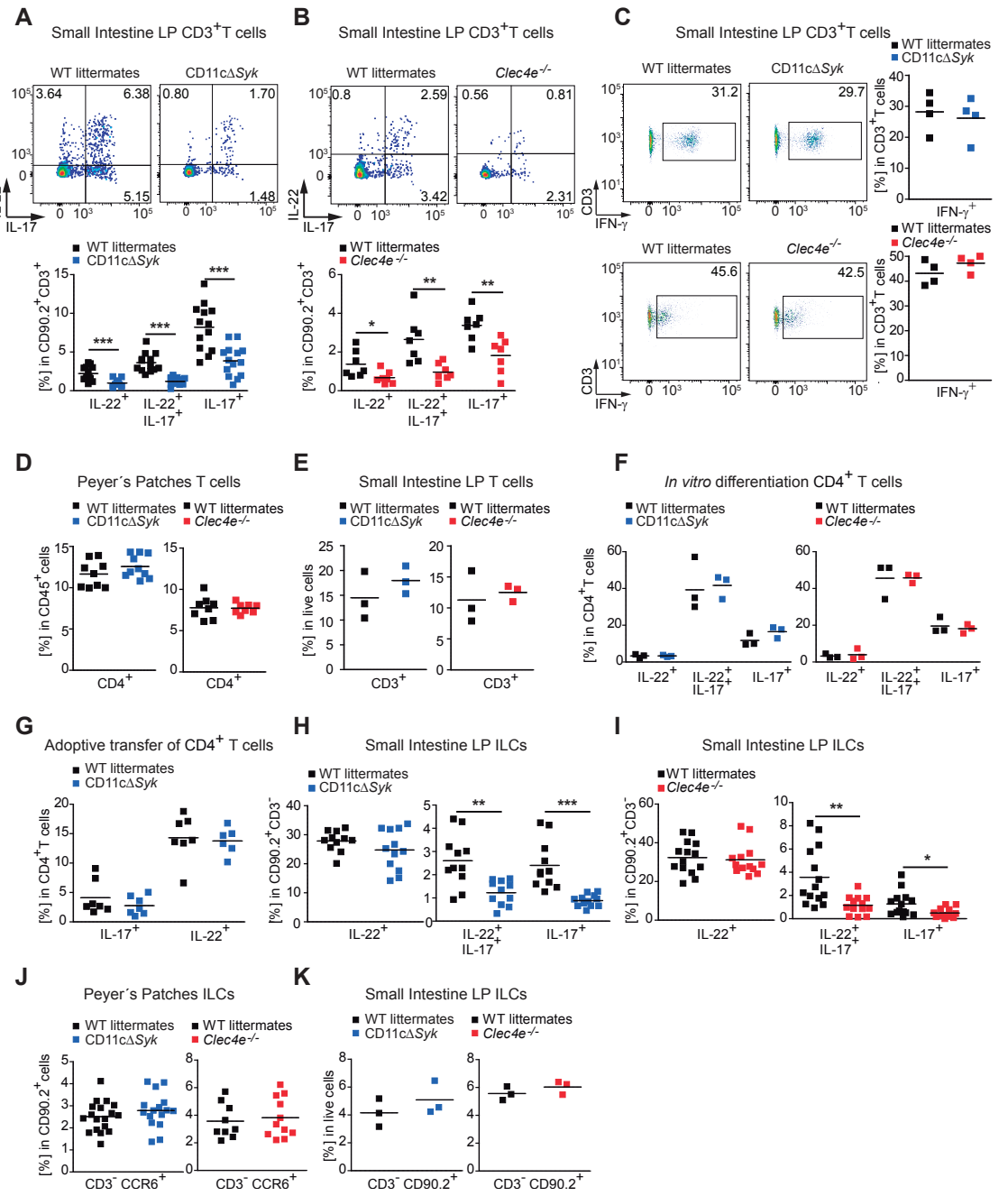

Figure S4. Mincle and Syk in DCs are needed for intestinal IL-17 and IL-22 steady state production. Related to Figure 4. (A-C) Representative plots and summary graph of IL-17, IL-22 (A,B) or IFN-γ (C) production after PMA and ionomycin stimulation in sorted CD3$^+$ T cells from small intestine LP of the indicated genotypes. (D) Summary graphs showing the frequencies of CD4$^+$ T cells from the PPs from CD11cΔ*Syk*, Mincle-deficient (*Clec4e*$^{-/-}$) mice and WT littermates. (E) Summary graphs of CD3$^+$ T cells from small intestine LP of the indicated genotypes. (F) IL-17 and IL-22 production by naive CD4$^+$ T cells from the indicated genotypes stimulated in vitro on plate-bound anti-CD3 and anti-CD28 under Th17 polarizing conditions for 5 days and restimulated for intracellular staining. (G) IL-22 and IL-17 production by intracellular staining of restimulated CD45.2$^+$ CD4$^+$ in the PPs 14 days after adoptive transfer of 6x10^6 naive CD4$^+$ T cells purified from CD45.2$^+$ WT and CD11cΔ*Syk* to CD45.1 recipients. (H, I) IL-17 and IL-22 basal production by intracellular staining of sorted CD3$^-$ CD90.2$^+$ ILCs from small intestine LP in the indicated genotypes. (J) Summary graphs of CD90.2$^+$CD3$^-$ CCR6$^+$ ILCs in the PPs in the indicated genotypes. (K) Summary graphs of CD3$^-$ CD90.2$^+$ ILCs from small intestine LP of the indicated genotypes. (A,B,D,G-J) Pool of two independent experiments. (C, E, F, K) One representative experiment of at least two performed is shown. * $p < 0.05$; ** $p < 0.01$; *** $p < 0.001$ (Unpaired two-tailed Student´s t test)

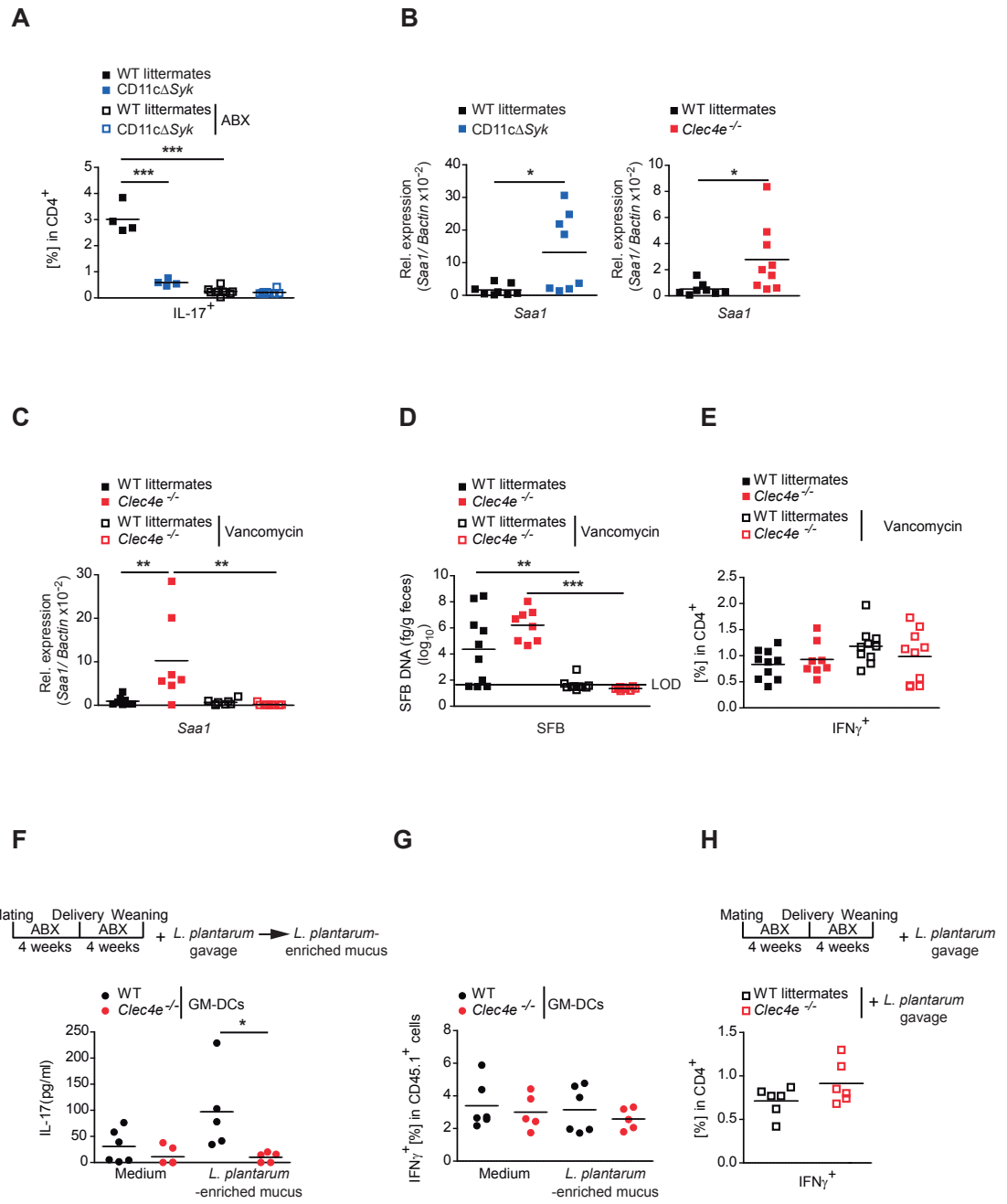

Figure S5. Commensal bacteria are required for Mincle-dependent Th17 generation in PPs. Related to Figure 5. (A) WT littermates and CD11cΔ*Syk* mice were treated with an antibiotic cocktail (ABX) containing ampicillin, neomycin, metronidazole and vancomycin in the drinking water during 4 weeks. Summary graph of IL-17 production after PMA and ionomycin stimulation in $CD4^+$ T cells from PPs determined by intracellular staining and flow cytometry. (B, C) *Saa1* transcripts were analyzed in the ileum of CD11cΔ*Syk*, Mincle-deficient (*Clec4e*$^{-/-}$) and WT littermate mice by qPCR and normalized to *β-actin* in steady state (B) or after vancomycin administration in the drinking water during 4 weeks (C). (D) SFB DNA was quantified by qPCR in feces from Mincle-deficient (*Clec4e*$^{-/-}$) and WT littermate in steady state or after vancomycin administration in the drinking water during 4 weeks. The lower line indicates the limit of detection (LOD). (E) Summary graph of IFN-γ production by intracellular staining after PMA and ionomycin stimulation in $CD4^+$ T cells from WT littermates and Mincle-deficient (*Clec4e*$^{-/-}$) mice treated with vancomycin as in (C). (F,G) Naive $CD45.1^+$ OVA-specific OTII T cells were co-cultured with sorted GM-DCs from WT and Mincle-deficient (*Clec4e*$^{-/-}$) mice loaded with $OVA_{323-339}$ peptide and pulsed or not (medium) with mucosal-associated commensals from WT mice treated with ABX during gestation and lactation and gavaged with *L. plantarum* at weaning (*L. plantarum*-enriched mucus; 10:1 DC ratio) (F) ELISA of IL-17 production by OTII cells from the co-cultures. (G) IFN-γ production after PMA and

ionomycin stimulation was measured by intracellular staining and flow cytometry in OT-II T cells from the co-cultures. (H) WT littermates and Mincle-deficient (*Clec4e*$^{-/-}$) mice treated with ABX during gestation and lactation and gavaged with *L. plantarum* at weaning ($1x10^6$) as indicated in the scheme (+ *L. plantarum* gavage). Summary graph of IFN-γ production by intracellular staining after PMA and ionomycin stimulation in $CD4^+$ T cells from PPs. (C-F) Pool of two independent experiments. (A,B,H) One representative experiment of at least two performed. * $p < 0.05$; ** $p < 0.01$; *** $p < 0.001$ (B) Unpaired two-tailed Student´s t test; (D) Two-tailed Mann-Whitney´s U test; (A,C,F) One-way ANOVA and Bonferroni post-hoc test.

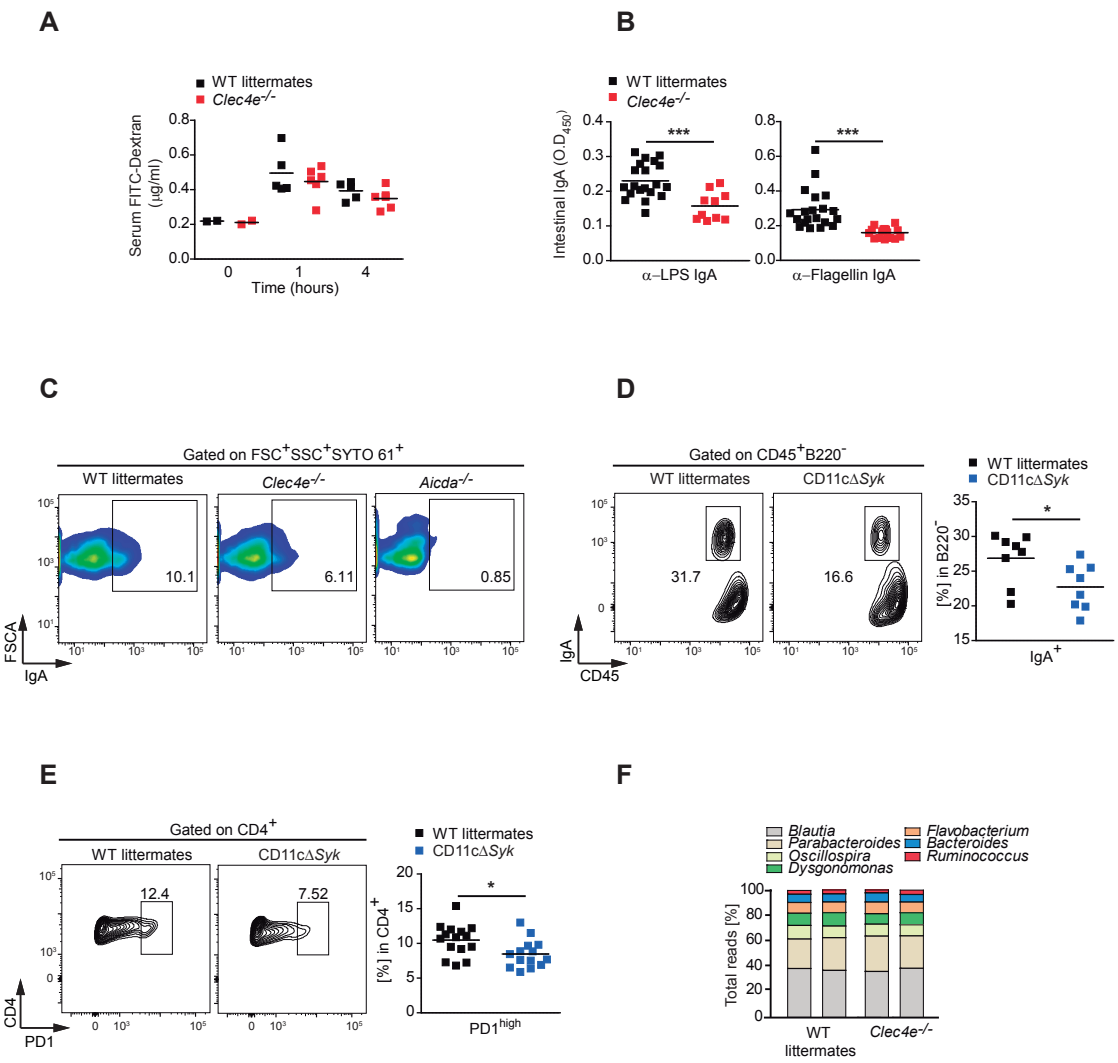

Figure S6. The Mincle-Syk axis contributes to the intestinal barrier function. Related to Figure 6. (A) Serum FITC-dextran concentrations measured by fluorimetry at 1 and 4 hours after administration by oral gavage to Mincle-deficient (*Clec4e*$^{-/-}$) and WT mice. (B) LPS-specific (left) and Flagellin-specific (right) IgA levels in the intestinal lumen of the indicated genotypes measured by ELISA. (C) Representative plots of IgA-coated bacteria, pre-gated on FSC^{+} SSC^{+} SYTO 61^{+} microbes. (D) Representative plot and summary graph of CD45^{+}B220^{-}IgA^{+} plasmatic cells from the small intestine LP of CD11cΔ*Syk* mice and WT littermate controls. (E) Representative plots and summary graph of CD4^{+}PD-1^{high} T cells from PPs of CD11cΔ*Syk* mice and their WT littermate controls. (F) 16S sequencing analysis of intestine luminal microbiota from Mincle-deficient (*Clec4e*$^{-/-}$) mice and their WT littermates. Graph showing the mean relative abundance of each genus in each sample (at least 10 mice pooled) from two independent experiments. (B, D, E, F) Pool of at least two independent experiments. (A, C) One representative experiment of at least two performed. * $p < 0.05$; *** $p < 0.001$ (Unpaired two-tailed Student´s t test).

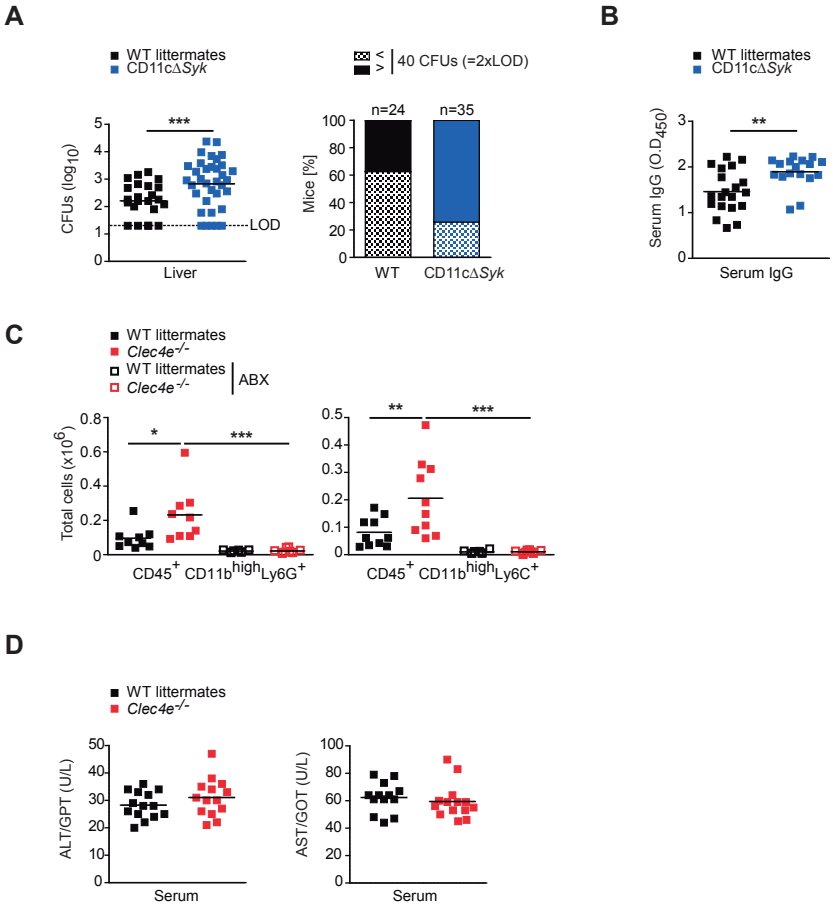

Metabolite	WT (gr.1)[a,b]	KO (gr. 2)[a,b]	Change (%) [c]	FC [c]	*p*-value
DAG (16:0/18:2)	44746 (19447)	36809 (14917)	+22	1.22	0.32 [e]
DAG (16:0/18:1)	79405 (40797)	60419 (23634)	+31	1.31	0.22 [e]
DAG (18:1/18:2)	49174 (26391)	37402 (21704)	+31	1.31	0.29 [e]
DAG (18:1/18:1)	104181 (62889)	77074 (42334)	+35	1.35	0.27 [e]
DAG (22:6/18:0)	18623 (5536)	14125 (5457)	+32	1.32	0.084 [e]
DAG (22:4/18:1) [d]	11389 (4071)	7767 (1885)	+47	1.47	**0.024** [e]
Myristic acid (C14:0) [g]	26445 (24000-290000)	309026 (21000-330000)	-91	0.086	0.44 [f]
Palmitic acid (C16:0) [g]	10071 (9200-11000)	8885 (8800-9700)	+13	1.13	0.052 [f]
Margaric acid (C17:0) [d]	450 (179)	211 (92)	+118	2.18	**0.0014** [e]
Linoleic acid (C18:2) [d, g]	873 (840-900)	755 (700-830)	+16	1.16	**0.019** [f]
Oleic acid (C18:1)	2660 (583)	2607 (549)	+2	1.02	0.84 [e]
Stearic acid (C18:0)	6084 (795)	5620 (703)	+8	1.08	0.18 [e]
Behenic acid (C22:0)	2295 (1243)	2180 (784)	+5	1.05	0.81 [e]
Total DAGs	307519 (149903)	233596 (102475)	+32	1.32	0.21 [e]
Total FFAs [g]	22743 (21000-24000)	20114 (19000-22000)	+13	1.13	0.075 [f]

Figure S7. Mincle-Syk pathway contributes to intestinal commensal microbiota containment. Related to Figure 7. (A) Bacterial translocation into the liver of CD11cΔ*Syk* and their respective WT littermates. Left: bacterial load as colony forming units (CFUs) per organ, indicating limit of detection (LOD). Right: Frequencies of mice of each genotype showing more than 40 CFUs per organ (=2xLOD). (B) ELISA of serum IgG against intestinal bacteria in the indicated genotypes. (C) Summary graph of $CD45^+$ $CD11b^{high}$ $Ly6G^+$ cells (left) or $Ly6C^+$ cells (right) infiltrated in the liver of Mincle-deficient (*Clec4e*$^{-/-}$) and their WT littermates in steady state or after administration of an antibiotic cocktail (ABX) containing ampicillin, neomycin, metronidazole and vancomycin in the drinking water during 4 weeks. (D) Alanine transaminase

(ALT/GPT) (left) and Aspartate transaminase (AST/GOT) (right) analyzed in serum of the indicated genotypes. (F) List of lipid species from diacylglycerides (DAG) and free fatty acids (FFA) classes identified in liver samples from Mincle-deficient (*Clec4e*$^{-/-}$) and their WT littermates. [a] Data as metabolites' abundance obtained from liver of ten animals/genotype from two independent experiments. [b] Data as mean and standard deviation; in non-normal distributed variable data, as median and interquartile range. [c] The change refers to *Clec4e*$^{-/-}$ mice compared with their WT littermates. [d] Significant metabolites (p-value < 0.05) for the comparison highlighted in bold. [e] Student t-test for normal distributed variables. [f] Mann−Whitney U-test for non-normal distributed variables. [g] Non-normal distributed data. FC, Fold Change. (A-E) Pool of at least two independent experiments. * $p < 0.05$; ** $p < 0.01$; *** $p < 0.001$(A, B) Unpaired two-tailed Student´s t test; (C) One-way ANOVA and Bonferroni post-hoc test.

Supplemental References

Conejero, L., Khouili, S. C., Martínez-Cano, S., Izquierdo, H. M., Brandi, P. & Sancho, D. 2017. Lung CD103+ dendritic cells restrain allergic airway inflammation through IL-12 production. *JCI Insight,* 2**,** e90420.

Goto, Y., Panea, C., Nakato, G., Cebula, A., Lee, C., Diez, M. G., Laufer, T. M., Ignatowicz, L. & Ivanov, I. I. 2014. Segmented filamentous bacteria antigens presented by intestinal dendritic cells drive mucosal th17 cell differentiation. *Immunity,* 40**,** 594-607.

Klindworth, A., Pruesse, E., Schweer, T., Peplies, J., Quast, C., Horn, M. & Glockner, F. O. 2013. Evaluation of general 16S ribosomal RNA gene PCR primers for classical and next-generation sequencing-based diversity studies. *Nucleic Acids Res,* 41**,** e1.

Martinez-Lopez, M., Iborra, S., Conde-Garrosa, R. & Sancho, D. 2015. Batf3-dependent CD103+ dendritic cells are major producers of IL-12 that drive local Th1 immunity against Leishmania major infection in mice. *Eur J Immunol,* 45**,** 119-29.

Matesanz, N., Nikolic, I., Leiva, M., Pulgarin-Alfaro, M., Santamans, A. M., Bernardo, E., Mora, A., Herrera-Melle, L., Rodriguez, E., Beiroa, D., Caballero, A., Martin-Garcia, E., Acin-Perez, R., Hernandez-Cosido, L., Leiva-Vega, L., Torres, J. L., Centeno, F., Nebreda, A. R., Enriquez, J. A., Nogueiras, R., Marcos, M. & Sabio, G. 2018. p38alpha blocks brown adipose tissue thermogenesis through p38delta inhibition. *PLoS Biol,* 16**,** e2004455.

Sancho, R., Nateri, A. S., De Vinuesa, A. G., Aguilera, C., Nye, E., Spencer-Dene, B. & Behrens, A. 2009. JNK signalling modulates intestinal homeostasis and tumourigenesis in mice. *EMBO J,* 28**,** 1843-54.

Snel, J., Heinen, P. P., Blok, H. J., Carman, R. J., Duncan, A. J., Allen, P. C. & Collins, M. D. 1995. Comparison of 16S rRNA sequences of segmented filamentous bacteria isolated from mice, rats, and chickens and proposal of "Candidatus Arthromitus". *Int J Syst Bacteriol,* 45**,** 780-2.

Vaishnava, S., Yamamoto, M., Severson, K. M., Ruhn, K. A., Yu, X., Koren, O., Ley, R., Wakeland, E. K. & Hooper, L. V. 2011. The antibacterial lectin RegIIIgamma promotes the spatial segregation of microbiota and host in the intestine. *Science,* 334**,** 255-8.

Zhao, X. Q., Zhu, L. L., Chang, Q., Jiang, C., You, Y., Luo, T., Jia, X. M. & Lin, X. 2014. C-type lectin receptor dectin-3 mediates trehalose 6,6'-dimycolate (TDM)-induced Mincle expression through CARD9/Bcl10/MALT1-dependent nuclear factor (NF)-kappaB activation. *J Biol Chem,* 289**,** 30052-62.

Zhao, Y., Gu, X., Zhang, N., Kolonin, M. G., An, Z. & Sun, K. 2016. Divergent functions of endotrophin on different cell populations in adipose tissue. *Am J Physiol Endocrinol Metab,* 311**,** E952-E963.